

Identification of Amino Acids of Sindbis Virus E2 Protein Involved in Targeting Tumor Metastases *in Vivo*

Alicia Hurtado, Jen-Chieh Tseng, Christopher Boivin, Brandi Levin, Herman Yee, Christine Pampeno, and Daniel Meruelo*

NYU Cancer Institute, Rita J. and Stanley H. Kaplan Comprehensive Cancer Center, and NYU Gene Therapy Center, New York University School of Medicine, 550 First Avenue, New York, NY 10016, USA

*To whom correspondence and reprint requests should be addressed. Fax: +1 212 263 8211. E-mail: daniel.meruelo@med.nyu.edu.

Available online 16 August 2005

Previous studies conducted in our laboratory with Sindbis viral vectors in animal models demonstrated excellent *in vivo* targeting of tumor cells and significant reduction of metastatic implant size. To explore the influence of Sindbis strain on these factors, we constructed new plasmids from the wild-type Ar-339 Sindbis virus strain and compared their sequences. We found differences in the replicase and envelope proteins between JT, HRSP, and Ar-339 sequences. We made chimeras combining both strains and studied their efficiency in SCID mice bearing tumor xenograft using IVIS *in vivo* imaging techniques. We found that JT envelope proteins targeted tumors more efficiently than those of Ar-339, while the Ar-339 replicase showed increased efficacy in tumor reduction. To determine which residues are responsible for tumor targeting, we made mutants of Ar-339 E2 envelope protein and tested them by IVIS imaging in ES-2 tumor-bearing and tumor-free mice. The change of only one amino acid from E70 to K70 in Ar-339 E2 suppressed the ability to target metastatic tumor implants in mice. A K70 and V251 double E2 mutant did not reverse the loss of targeting capability. Only the mutant with JT E2 and Ar-339 helper targeted tumor, though with less intensity.

Key Words: Sindbis virus vector, ovarian cancer, tumor targeting, *in vivo* imaging

INTRODUCTION

Sindbis virus, a member of the alphavirus genus in the *Togaviridae* family, is a single-stranded, enveloped, positive-strand RNA virus [1]. In nature, it is transmitted via mosquito bites to mammals. Thus Sindbis virus evolved as a blood-borne vector. This hematogenous delivery property enables Sindbis vectors to reach tumor cells throughout the body [2,3]. With the aim of broadening the knowledge of Sindbis vector mechanisms for cancer gene therapy, our lab has been studying two different kinds of Sindbis vectors, SP6-H/SP6-R, that come from wild-type Ar-339 and JT-BB/JT-Rep from an Ar-339 laboratory-adapted strain, Toto1101. Sindbis virus Ar-339 was first isolated in August 1952 from a pool of mosquitoes (*Culex pipiens* and *C. univittatus*) trapped in the Egyptian Sindbis district [4–6]. Toto1101 was obtained from the heat-resistant (HR) strain initially derived from Ar-339 [7]. The first studies done with JT vectors in animal models showed good targeting of tumor cells and significant reduction of metastatic implant size [8]. Further studies of these vectors in tumor-bearing SCID mice were done using the new

technique of the IVIS Imaging System, which allows *in vivo* monitoring of viral vector luciferase activity and tumor cells in parallel. In tumor-induced SCID mice there was a very significant correlation between the locations of vectors and tumor cells [2]. Sindbis vector targeting *in vivo* leads to marked reduction of tumor growth and increased survival. Despite these very promising results for the gene therapy of cancer, complete survival of mice in several tumor models has not yet been achieved.

In an effort to seek improvements to the vector, we made two new plasmids from wild-type Sindbis virus and explored combinations of the helper and replicase segments of both strains (JT-BB/SP6-R, SP6-H/JT-Rep, SP6-H/SP6-R, JT-BB/JT-Rep). Using these new vectors we studied tumor size reduction and mouse survival in a SCID mouse ovarian cancer xenograft model. Unexpectedly, we found that those vectors carrying Ar-339 helper (SP6-H) were less efficient in targeting tumors than the JT vectors and that those carrying Ar-339 replicase (JT-BB/SP6-R and SP6-H/SP6-R) were more efficient in tumor reduction. As the main differences between JT and Ar-339 sequences were found in the E2 envelope protein, in this study we

focused on tumor targeting by utilizing the two strains and E2 envelope protein mutants to identify the responsible amino acids.

RESULTS AND DISCUSSION

HRSP versus Ar-339 Sequence Analysis

To obtain the vectors desired for our studies, we first amplified Ar-339 virus in chicken embryo fibroblasts (CEF) and cloned cDNA into sequencing plasmids as six separate overlapping fragments. cDNA-3 and cDNA-4 overlap the 312-bp fragment (nt 7334–7646) containing the viral subgenomic promoter. We compared the Ar-339 sequence obtained to the small plaque variant of the HR strain (HRSP) Sindbis sequence [9] and to the sequence of Sindbis plasmids, JT-BB and JT-Rep, used previously in our laboratory to produce JT viral vectors [3]. Results are shown in Table 1. In the viral replicase (nsP1–nsP4), comparing the HRSP map with Ar-339, we found three point mutations in nsP1: nt 353, a silent mutation, and nt 1380 and 1381, which both change amino acid 441 from Cys to Ile in Ar-339. This mutation is not within the carboxy-terminal domain required for enzymatic activity [10]. nsP2 has three mutations compared to the HRSP sequence, one silent at nt 673 (A to G) and two (nt 2992 and 3579) that change amino acids 438 (Pro to Leu) and 634 (Lys to Glu), respectively. Both amino acids are outside the active helicase and protease domains of nsP2 [11]. In nsP4 there was only a silent mutation at nt 7337 (T to C).

The Ar-339 capsid protein had two mutations compared with the HRSP sequence, one silent at nt 8345 (C to A) and one at nt 7846 that changed Pro 67 to Gln. This change is in the amino acid 11 to 74 region, which does not bind to Sindbis RNA [12], and is not in the capsid protein interaction domains, residues 36–39, 108–111, 172, 180–183, 201, 231–234, 240, or 254 [13,14].

There were also two silent mutations in E1 at nt 10392 (T to C) and 10469 (T to A), and two differences in the Ar-339 with the HRSP map were found at positions Ala 72 to Val and 237 (Ser to Ala) in Ar-339, which are both located in domain II. Residues of this domain are involved in E1–E1 interaction in the virus spike [15].

Most of the coding changes were in the envelope protein E2, in which the antigenic sites and the binding receptor domain of the virus have been described. Comparing the HRSP sequence with Ar-339, we found five amino acid changes located in the external leaf-like domain of the E2 protein, which includes the amino terminus to residue 218 [15]. Changes found are in amino acids 3 (Ile to Thr), 23 (Val to Ala), and 70 (Lys to Glu) and two mutations, 172 (Arg to Gly) and 181 (Glu to Lys), occur in the putative receptor-binding domain (amino acids 170 to 220). We found no changes in the endodomain that interacts with the capsid protein (from 391 to 483) or with the E2–E1 interaction region.

JT versus Ar-339 Sequence Analysis

Sequence analysis of cloned Ar-339 and comparison with JT vector has been an important tool for the discovery of

TABLE 1: Nucleotide differences between Ar-339 and JT vectors and Sindbis virus HRSP

nt ^a	Protein	JT	HRSP	Ar-339	HRSP → Ar339	HRSP → JT	JT → Ar339
353	nsP1 (98)	C	C	T	UAC(Y) _ UAU(Y)	UAC(Y) _ UAC(Y)	UAC(Y) _ UAU(Y)
1380-1	nsP1 (441)	TG	TG	AT	UGC(C) _ AUC(I)	UGC(C) _ UGC(C)	UGC(C) _ AUC(I)
2992	nsP2 (438)	T	C	T	CCC(P) _ CUC(L)	CCC(P) _ CUC(L)	CUC(L) _ CUC(L)
3579	nsP2 (634)	G	A	G	AAA(K) _ GAA(E)	AAA(K) _ GAA(K)	GAA(E) _ GAA(E)
3698	nsP2 (673)	A	G	G	AAG(K) _ AAG(K)	AAG(K) _ AAA(K)	AAA(K) _ AAG(K)
5702	nsP3 (534)	T	A	A	CCA(P) _ CCA(P)	CCA(P) _ CCU(P)	CCU(P) _ CCA(P)
7337	nsP4 (529)	T	T	C	GAU(D) _ GAC(D)	GAU(D) _ GAC(D)	GAU(D) _ GAC(D)
7846	Capsid (67)	C	C	A	CCG(P) _ CAG(Q)	CCG(P) _ CCG(P)	CCG(P) _ CAG(Q)
8009	Capsid (121)	A	G	G	GAG(Q) _ GAG(E)	GAG(Q) _ GAA(Q)	GAA(Q) _ GAG(Q)
8345	Capsid (233)	C	C	A	GGC(G) _ GGA(G)	GGC(G) _ GGC(G)	GGC(G) _ GGA(G)
8638	E2 (3)	T	T	C	AUU(I) _ ACU(T)	AUU(I) _ AUU(I)	AUU(I) _ ACU(T)
8698	E2 (23)	A	T	A	GUA(V) _ GCA(A)	GUA(V) _ GCA(A)	GCA(A) _ GCA(A)
8838	E2 (70)	A	A	G	AAG(K) _ GAG(E)	AAG(K) _ AAG(K)	AAG(K) _ GAG(E)
9144	E2 (172)	G	A	G	AGA(R) _ GGA(G)	AGA(R) _ GGA(G)	GGA(G) _ GGA(G)
9171	E2 (181)	G	G	A	GAA(E) _ AAA(K)	GAA(E) _ GAA(E)	GAA(E) _ AAA(K)
9382	E2 (251)	T	C	C	GCC(A) _ GCC(A)	GCC(A) _ GUC(V)	GCC(A) _ GUC(V)
10279	E1 (72)	C	C	T	GCU(A) _ GUU(V)	GCU(A) _ GCU(A)	GCU(Ala) _ GUU(V)
10288	E1 (75)	G	A	A	GAC(D) _ GAC(D)	GAC(D) _ GGC(G)	GGC(G) _ GAC(D)
10392	E1 (109)	T	T	C	UUG(L) _ CUG(L)	UUG(Leu) _ UUG(L)	UUG(L) _ CUG(L)
10469	E1 (133)	T	T	A	AUU(I) _ AUA(I)	AUU(I) _ AUU(I)	AUU(I) _ AUA(I)
10773	E1 (237)	T	T	G	UCA(S) _ GCA(A)	UCA(S) _ UCA(S)	UCA(S) _ GCA(A)

Codon changes are in boldface.

^a Nucleotide numbers follow HRSP sequence (Accession No. NC_001547.1 [9]).

E2 amino acids involved in targeting tumor metastases *in vivo*. We found only one mutation in the replicase, Cys 441 to Ile of Ar-339 nsP1. In the structural proteins there were a total of eight differences, only one in the capsid protein, Pro 67 to Gln in Ar-339. Three mutations in the E1 envelope protein (Ala 72 to Val, Gly 75 to Asp, and Ser 237 to Ala) were located in E1–E1 interaction domain II. E1 Asp 75 and Ala 237 of Ar-339 are highly conserved in the Sindbis-like alphaviruses; all viruses in this group carry E1 Asp 75. There is no virus in the group that has serine at 237, which occurs only in the JT sequence. These data suggest that E1 Gly 75 and Ser 237 of JT-BB plasmid could more likely be point mutations that arose in our laboratory strain.

Most of the differences were in the E2 protein: three in the leaf-like domain, Ile 3 to Thr, Lys 70 to Glu, and Glu 181 to Lys, and one in the ectodomain, Ala 251 to Val. Position 251 is important for virus maturation in CEF [16]. We found the changed amino acids of the JT and Ar-339 vectors versus the HRSP strain mainly in the viral spike, although in different residues, suggesting a different evolutionary lineage of both strains. We studied the roles of these E2 spike mutations in our mouse tumor models *in vivo*.

Colocalization

From cloned Ar-339 virus we engineered two plasmids, SP6-R carrying the virus replicase and SP6-H containing viral capsid and envelope proteins. To measure the degree and specificity of Ar-339 Sindbis infection of tumor cells, we performed IVIS imaging studies that measured independent bioluminescent signals from tumor cells and vector C (SP6-H/SP6-RhRluc). The ES-2/Fluc cells expressed the firefly luciferase gene (Fluc), which uses D-luciferin as substrate, and the vector carried a different luciferase gene cloned from soft coral *Renilla reniformis* (hRluc), which uses coelenterazine to generate bioluminescence. The two luciferases are highly substrate specific and do not cross-react [17]. First we treated each anesthetized mouse with coelenterazine and collected the image (Fig. 1A, left), and then we treated with D-luciferin for sequential IVIS imaging of ES-2/Fluc cells (Fig. 1A, right). We quantitated the bioluminescence signals generated in the same animal from vector and ES-2/Fluc using Living Image software. We gridded the images of Rluc and Fluc signals (12 × 8, 96 boxed regions) and analyzed corresponding regions for statistical correlation (Fig. 1B). A highly significant correlation was established ($P < 0.0001$), indicating that a single intraperitoneal (ip) delivery of Ar-339 Sindbis vector leads to very efficient infection of the metastasized tumor cells throughout the peritoneal cavity. In several mice we observed an additional infection outside the peritoneal cavity. To assess if this was due to nonspecific vector infection and if this would compromise vector safety, we performed the Ar-339 targeting experiment (see below).

Disease Progression

To compare the ability of Sindbis vectors Ar-339 and JT in targeting and suppression of disease, we constructed chimeric vectors and tested them in the ES-2/Fluc mouse metastatic ovarian cancer model described previously [3]. We injected five female SCID mice per vector group ip with 1.5×10^6 ES-2/Fluc cells (day 0) and imaged them with IVIS the next day to verify the presence of ES-2/Fluc cells in the mice. We let the cells grow for 4 days before starting daily treatment with vectors. There were five groups of animals, one of which did not receive vector treatment; the remaining four were injected with vectors carrying *Renilla* luciferase as reporter gene: A (JT-BB/SP6-RhRluc), B (SP6-H/JT-RephRluc), C (SP6-H/SP6-RhRluc), and D (JT-BB/JT-RephRluc). Viral vectors and the plasmids used to engineer them are summarized in Table 2.

As the main purpose of this experiment was to study the differences in tumor targeting of these viral vectors *in vivo*, we titered the vectors in the same cell line used to induce the tumors, ES-2/Fluc, and standardized these functional titers for all of them at 10^6 transducing units (TU)/ml. Although this *in vitro* equivalent titer does not quantitatively indicate equivalent viral particles of the vectors in each dose, it provides the functional uniformity of vector particles that are able to target ES-2/Fluc cells and is, therefore, therapeutically relevant.

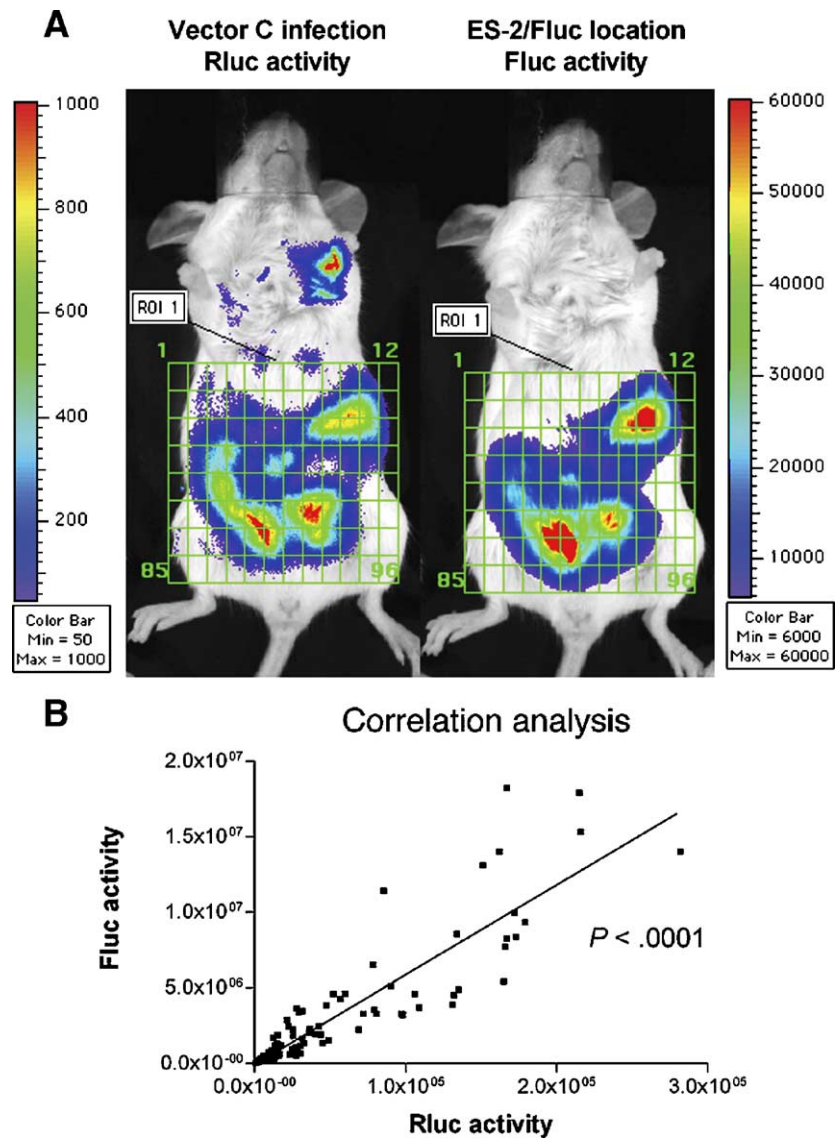
We determined total whole-body photon counts by IVIS imaging on days 1, 5, 13, and 19 to determine disease progression of ES-2/Fluc metastases. We also compared survival curves (Fig. 2). Mice treated with vectors carrying Ar-339 replicase (A and C) showed greater reduction. The change from polar Cys in JT to an aliphatic residue, Ile 441, in Ar-339, while not within the catalytic domain, could play a role in enhancing replicase activity *in vivo*.

Examining the structural proteins for tumor targeting, vector A was more efficient in reducing tumor progression and resulted in better survival of the mice, indicating that JT-BB is more efficient. Though both structural proteins and replicase function efficiently in vectors *in vivo*, the data suggested that the use of Ar-339 replicase (SP6-R) would be preferable with the best targeting vectors, increasing the efficiency of tumor kill through increased replicase-associated effects.

Ar-339 Targeting

To analyze tissues or organs targeted by the Ar-339 strain, we made new chimeric vectors with firefly luciferase as the reporter gene, since its stronger bioluminescent signal allows the study of vectors in animal organs. We tested each vector in two groups of five SCID female mice: tumor-free and injected with ES-2 cells. To assess which component of the C vector was responsible for the chest bioluminescence, we made three Fluc chimeric vectors: A (JT-BB/SP6-RFluc), B (SP6-H/JT-

FIG. 1. Colocalization in peritoneal cavity of vector C. (A) Vector C infection colocalized with the metastasized ES-2/Fluc tumors in the peritoneal cavity as determined by the IVIS Imaging System. SCID mice were inoculated ip with 1.5×10^6 ES-2/Fluc cells. Five days later, while the disease was still microscopic, inoculated mice received a single ip treatment of vector C and were imaged the next day. The first IVIS imaging was done by ip injection of Rluc substrate, coelenterazine, followed by a 5-min acquiring interval (left). Thirty minutes after the coelenterazine injection, when the short-lived Rluc signals had faded away, Fluc substrate, D-luciferin, was injected ip to determine the ES-2/Fluc tumor locations (right). (B) Correlation analysis of vector C shows a high correspondence between tumor cells and vector infection in the peritoneal cavity.



RepFluc), and C (JT-BB/JT-RepFluc). The vector titers in ES-2 cells were 10^4 TU/ml for vector A and 10^3 TU/ml for vectors B and C.

TABLE 2: Summary of Sindbis vectors

Viral vector	Helper plasmid	Replicon plasmid
A	JT-BB ^a	SP6-R ^b
B	SP6-H ^b	JT-Rep ^a
C	SP6-H	SP6-R
D	JT-BB	JT-Rep
Mut-1	SP6-HK70	SP6-R
Mut-2	SP6-HK70V251	SP6-R
Mut-4	SP6-HI3K70E181V251	SP6-R

^a JT Sindbis virus strain.

^b Ar-339 Sindbis virus strain.

Tumor-free mice received one dose of vector at day 0 and were IVIS-imaged next day (Fig. 3A). All three groups showed a low background signal in fat tissue. Two of 10 mice, 1 in the vector B and 1 in the vector C group, showed some additional bioluminescent signal in the chest, as previously observed in the colocalization experiment (Fig. 1, left). To investigate if vectors were infecting organs in these mice, we IVIS-imaged the intraperitoneal cavity and harvested organs separately. The chest signal observed corresponded to connective tissue in the ribs, while organs had no background signal (Fig. 3). To study if repeated doses could lead to a cumulative infection in tumor-free mice, we injected a second dose ip on day 2 and repeated the imaging on day 3. The results (Fig. 3B) showed low background signal in fat tissue for vectors B and C and no signal at all for vector A, indicating that the

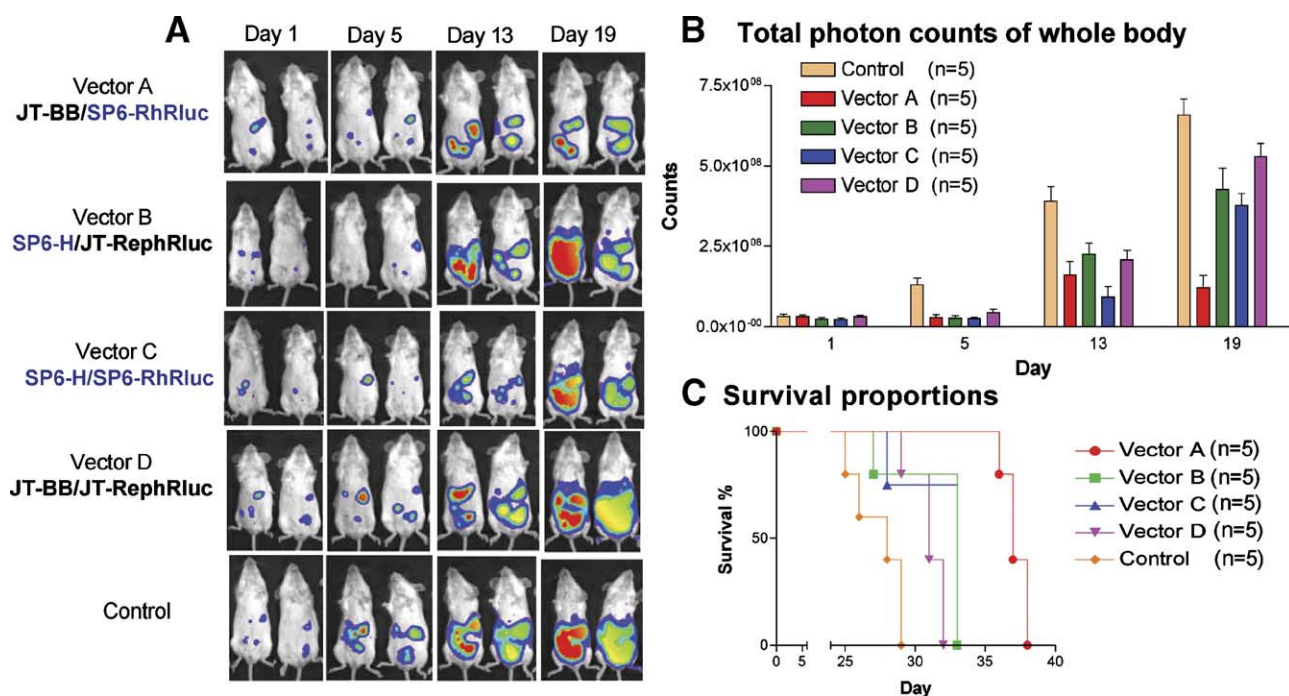


FIG. 2. Suppression of disease progression by Ar-339 and JT chimeric vectors. (A) ES-2/Fluc cells (1.5×10^6) were inoculated ip into SCID mice on day 0. Next day (day 1), mice were imaged using the IVIS Imaging System with D-luciferin as substrate and were split into five groups of five mice each: control, which received no vector treatment; vector A; vector B; vector C; and vector D. The groups received daily ip treatments of corresponding Sindbis vectors (10^6 TU) and were IVIS-imaged on days 1, 5, 13, and 19 after the start of treatment. All vector treatments suppressed the tumor growth on the mesentery and diaphragm and reduced the signals on the omentum compared with control mice. Image scale min 8×10^3 , max 10^5 counts/pixel. (B) Quantitative analysis of the whole-body total photon counts of control and Sindbis-treated mice. Error bars represent the SEM. (C) Survival curve of mice.

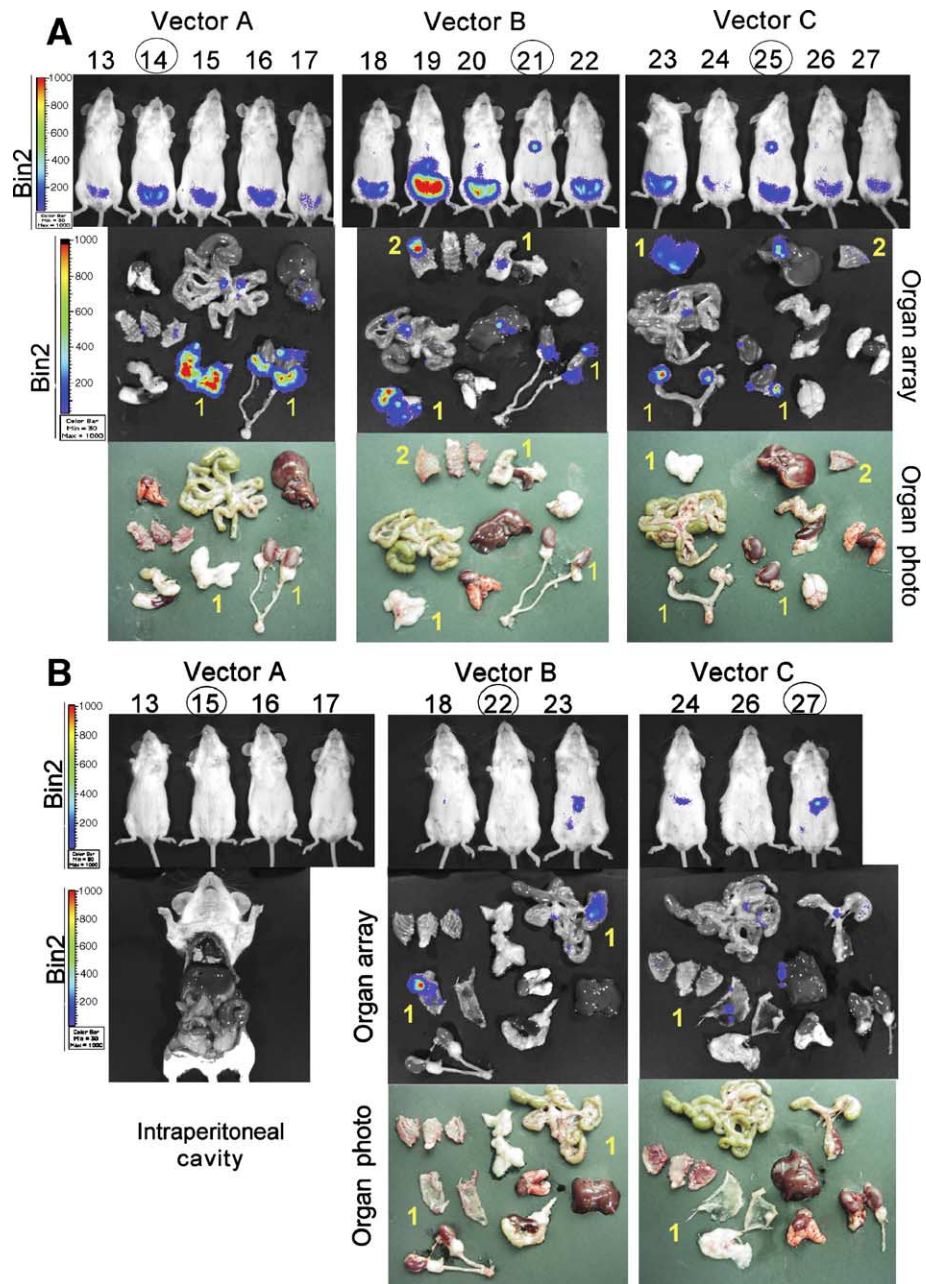
background is transient and does not affect the target effectiveness of Ar-339 vectors in repeated treatments.

Previous studies of JT/Fluc vector in 5-day ES-2 tumor-induced mice showed that the vector specifically targets metastasized ES-2 cells after one injection and also in a second dose 2 days later [2]. To study if the difference between sequences could affect the specificity of Ar-339 vector, we tested these three chimeric vectors in the same model. Mice injected with 2×10^6 ES-2 cells on day 0 received one ip dose of vectors on day 5 (10^4 TU/ml) and were IVIS-imaged on day 6. We imaged the peritoneal cavity and organs of two mice per group. For all vectors the bioluminescence shown in the organ array (Fig. 4A) correlates with the visible ES-2 metastatic tumor implants. To verify the tissue infected by the vectors we performed hematoxylin and eosin (H&E) and immunohistochemical staining on isolated tumors for luciferase. The H&E of the tumor implant on peritoneal adipose tissue of mouse 31 treated with vector A (Fig. 4C) showed a hypercellular tumor population with a central area of nonviable tumor and acute inflammation. A consecutive 5- μ m section of the tissue was stained with an antibody specific to luciferase. No adipose tissue or nonviable tumor was stained, only viable tumor cells had specific signal. We observed similar immunohistochemical

results in other tumor implants analyzed, indicating highly specific targeting by the vectors. On day 7 two mice per group received a second ip dose of vector and one mouse was not injected to serve as a luciferase background signal control (Fig. 4B). Vector A showed a similar signal compared with previous doses, but vectors carrying Ar-339 structural proteins, B and C, showed decreased bioluminescence signals in tumors compared with the first injection. The difference in reinfection suggests that amino acid changes in the structural proteins may play an important role in targeting metastases during repetitive treatment with vector.

To ascertain which mutations were critical for the vector-targeting properties, we generated a chimeric vector, QE2, which contains E2 from JT-BB and the remaining structural proteins from Ar-339. Comparing QE2 and Ar-339 vectors in the same IVIS animal model, we observed, in tumor-free animals, low background in fat tissue with the first dose and no signal in the second dose. In ES-2 5-day induced-tumor mice, vector QE2 was able to target tumor and was able to reinfect animals, though the bioluminescent signal was not as strong as for the Ar-339 vector (data not shown). This indicated that the Ar-339 sequence in the E2 envelope protein was primarily responsible for the targeting pattern, though

FIG. 3. Background infection of Ar-339 and JT chimeric vectors. (A) Five SCID female tumor-free mice per group were injected ip on day 0 with one dose of vector A (JT-BB/SP6-RFluc), vector B (SP6-H/JTRepFluc), or C (SP6-H/SP6-RFluc) and the next day (day 1) IVIS-imaged for vector luciferase signal. The peritoneum from the mice indicated with a circled number was removed and the organs were harvested and imaged (rows 2 and 3). All vectors showed infection in fat tissue (1), and in the vector B and C groups two mice showed a low background signal on ribs (2) but not in organs. (B) The remaining mice per group received a second ip injection of the vectors on day 2 and were IVIS-imaged on day 3. The peritoneal cavities and organs correspond to the circled mice. Image resolution Bin2, scale min 30, max 10^3 counts/pixel for all images.



the optimal amino acid arrangement was still not clear. To address this question we performed site-directed mutagenesis on the Ar-339 E2 envelope protein.

E2 Mutants

In E2 there are four amino acid differences between JT and Ar-339 strains that are located at positions 3, 70, 181, and 251 (Table 1). We generated three E2 mutants in these residues, Mut-1, Mut-2, and Mut-4 (Table 2), and tested them in tumor-free and ES-2 5-day induced-tumor mice as previously described for vectors A, B, and C. E2

Lys 70 is implicated in BHK specificity [18] and residues 69 to 72 have been related to targeting of vertebrate cells [19,20]; to analyze the implication of this residue in tumor targeting the three point mutants contain Lys at position 70. In Mut-1 only Ar-339 Glu 70 was changed to Lys. Amino acid 251 of E2 is highly conserved between different Sindbis isolates [21] and mutation to valine at this position has been related to host-range phenotype [16]. To explore the possible effects of this amino acid combined with residue 70, we made Mut-2, which has Lys 70 and also Ar-339 Ala 251 mutated to Val. Residues

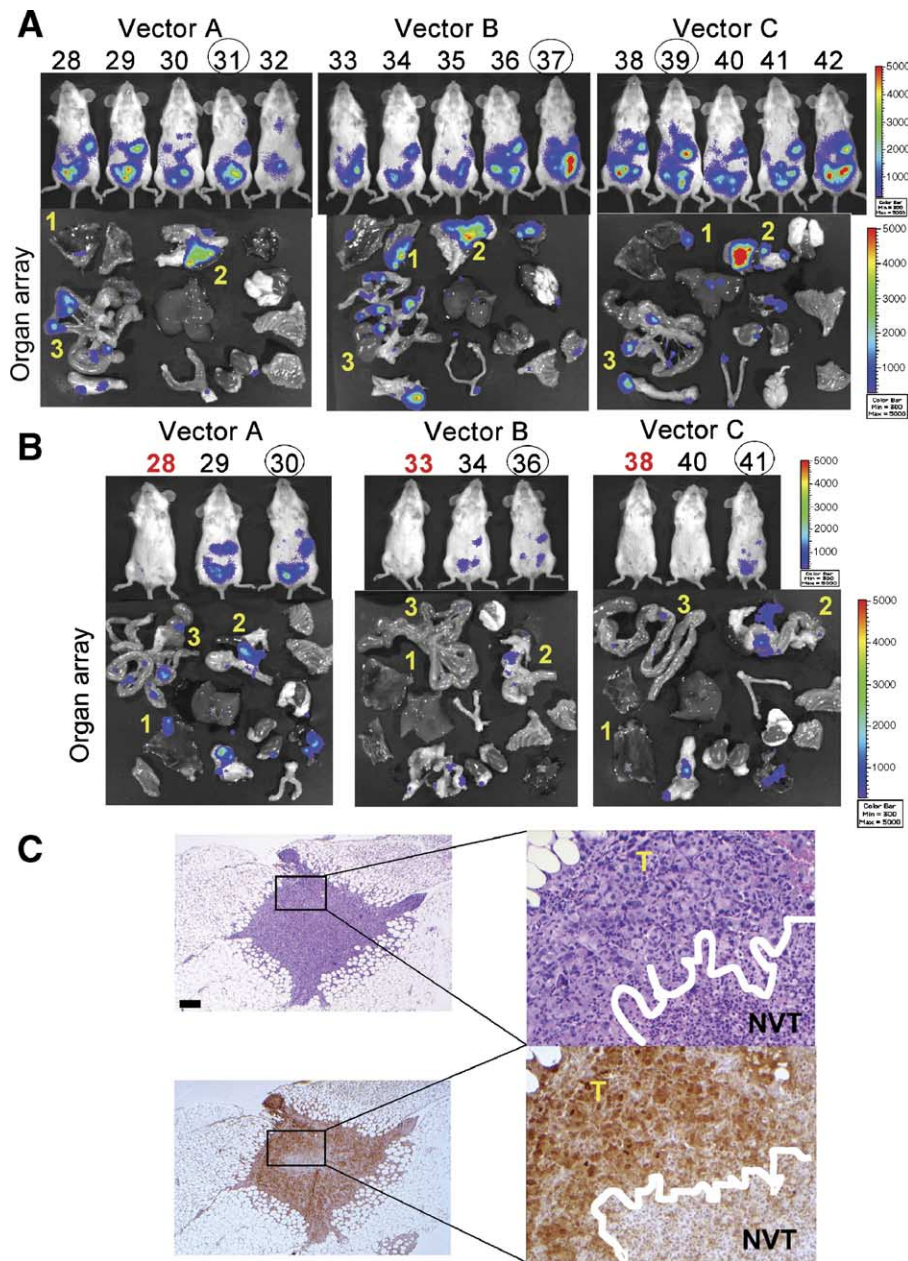


FIG. 4. Tumor targeting of Ar-339 and JT chimeric vectors. (A) SCID female mice were injected ip on day 0 with 2×10^6 ES-2 cells/mouse. On day 4 five mice per group were injected ip with one dose of vector A (JT-BB/SP6-RFluc), vector B (SP6-H/JTRepFluc), or vector C (SP6-H/SP6-RFluc) and the next day (day 5) IVIS-imaged for vector luciferase signal. The peritoneum from the mice with circled numbers was removed and the organs were harvested and imaged. All vectors targeted tumor implants. Tumors on peritoneum (1), pancreas-omentum (2), and bowel (3) are indicated. (B) Some mice per group received a second ip injection of the vectors of day 6, and the organs of the circled mice (bottom rows) were IVIS imaged on day 7. One mouse per group (Nos. 28, 33, 38) was not injected to serve as luciferase background control. For both A and B the image scale for whole body is min 30, max 10^3 counts/pixel, scale for organ array is min 300, max 5×10^3 counts/pixel. (C) Staining of tumor sections with antibody specific for luciferase confirmed tumor targeting of vector. H&E staining of isolated tumor implants of the peritoneal adipose tissue (upper images) shows a hypercellular tumor population (T) with a central area composed of nonviable tumor and acute inflammation (below white line NVT). Immunohistologic staining of consecutive 5- μ m tumor sections with antibody specific for luciferase shows intense stain of the tumor but not of the areas with the inflammatory cells (lower images). Right side corresponds to higher magnification of boxed regions on left. Bar, 100 μ m.

at positions 3 and 181 are located in the external leaf-like domain of E2 protein and, more specifically, 181 is in the receptor-binding domain. To assess if the combination of the four amino acid changes in the E2 is responsible for the difference in infection of Ar-339 vectors, we made mutant Mut-4, with Lys 70, Val 251, Ile 3, and Glu 181. To ensure that the differences in signals were due to the E2 mutations, all five vectors tested carried the same replicase SP6-RFluc: vector A (JT-BB/SP6-RFluc), C (SP6-H/SP6-RFluc), Mut-1 (SP6-HK70/SP6-RFluc), Mut-2 (SP6-HK70V251/SP6-RFluc), and Mut-4 (SP6-HI3K70E181V251/SP6-RFluc). We titered the

vectors in ES-2 cells; the functional titers were 10^5 TU/ml for vector A, 10^3 TU/ml for vectors C and Mut-1, and 10^4 TU/ml for Mut-2 and Mut-4.

In tumor-free mice vectors A and C gave infection background in some of the animals, with only one of the five vector C mice showing a low bioluminescent signal in the ribs (Fig. 5A). With second doses of these vectors the background was even less noticeable (Fig. 5B). Mut-1 and Mut-2 did not produce background bioluminescent signal at either dose. Mut-4 showed barely detectable signal in fat tissue, much less intense than that of vectors A and C. Only using high-sensitivity Bin10 resolution was

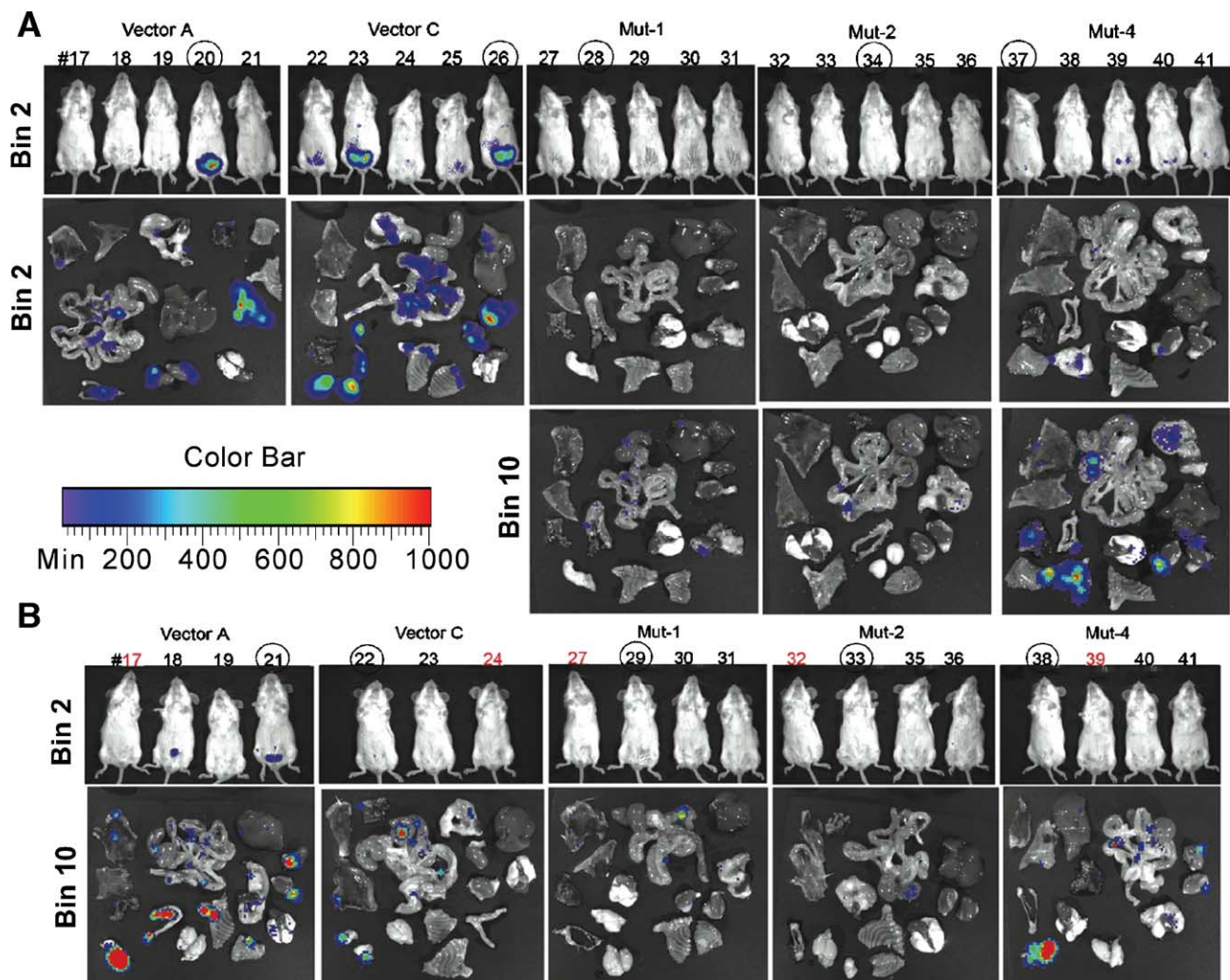


FIG. 5. Background infection of Ar-339 E2 mutants. (A) Five SCID female tumor-free mice per group were injected ip on day 0 with one dose of vector A (JT-BB/SP6-RFluc), vector C (SP6-H/SP6-RFluc), Mut-1 (SP6-HK70/SP6-RFluc), Mut-2 (SP6-HK70V251/SP6-RFluc), or Mut-4 (SP6-HI3K70E181V251/SP6-RFluc). Next day, the mice were IVIS-imaged for vector luciferase signal. The peritoneum was removed and the organs were harvested and IVIS-imaged. E2 mutant organ arrays were also IVIS-imaged at Bin10 resolution to increase the detection limit (bottom row). (B) Some mice per group received a second ip injection of the vectors on day 2, and organs were harvested and IVIS imaged. Circled mice (Nos. 17, 24, 27, 32, and 39) were not injected to serve as luciferase background controls. Image scale for Bin2 whole mouse is min 30, max 10^3 , organs Bin2 and Bin10 min 20, max 10^3 counts/pixel. Organs correspond to circled mice.

low bioluminescence signal detected in mice 21, 22, and 38 of vector groups A, C, and Mut-4, respectively.

In ES-2 tumor-induced mice we observed a dramatic decrease in the infectivity of mutants Mut-1 and Mut-2 and a significant reduction in Mut-4 after the first and second dose (Figs. 6A and 6B). Thus, the change of only one amino acid in Ar-339 E2 at position 70 makes vector C lose the specificity in targeting ES-2 tumor metastases *in vivo*. The double mutant with Lys 70 and Val 251, Mut-2, does not revert the vector tropism. Mut-4 combines vector JT E2 with Ar-339 E1, E3, and capsid sequences. The fact that Mut-4 could not revert to full infectivity indicates

that the interaction between E2 and E1 in the vector spike could also play an important role in vector targeting.

The change in polarity and charge of the E2 70 amino acid, common in the three mutants, would alter the conformation of the spike and may consequently affect the cell binding properties of the vector. Another possibility that could explain the loss of tumor targeting *in vivo* would be a reduced stability of the vector in mice. Alignment of protein sequences among 17 different viruses of the Sindbis-like alphavirus group shows that 10 of the 17 have a gap in Sindbis E2 residues 68–71, including Semliki Forest virus, which has a structure

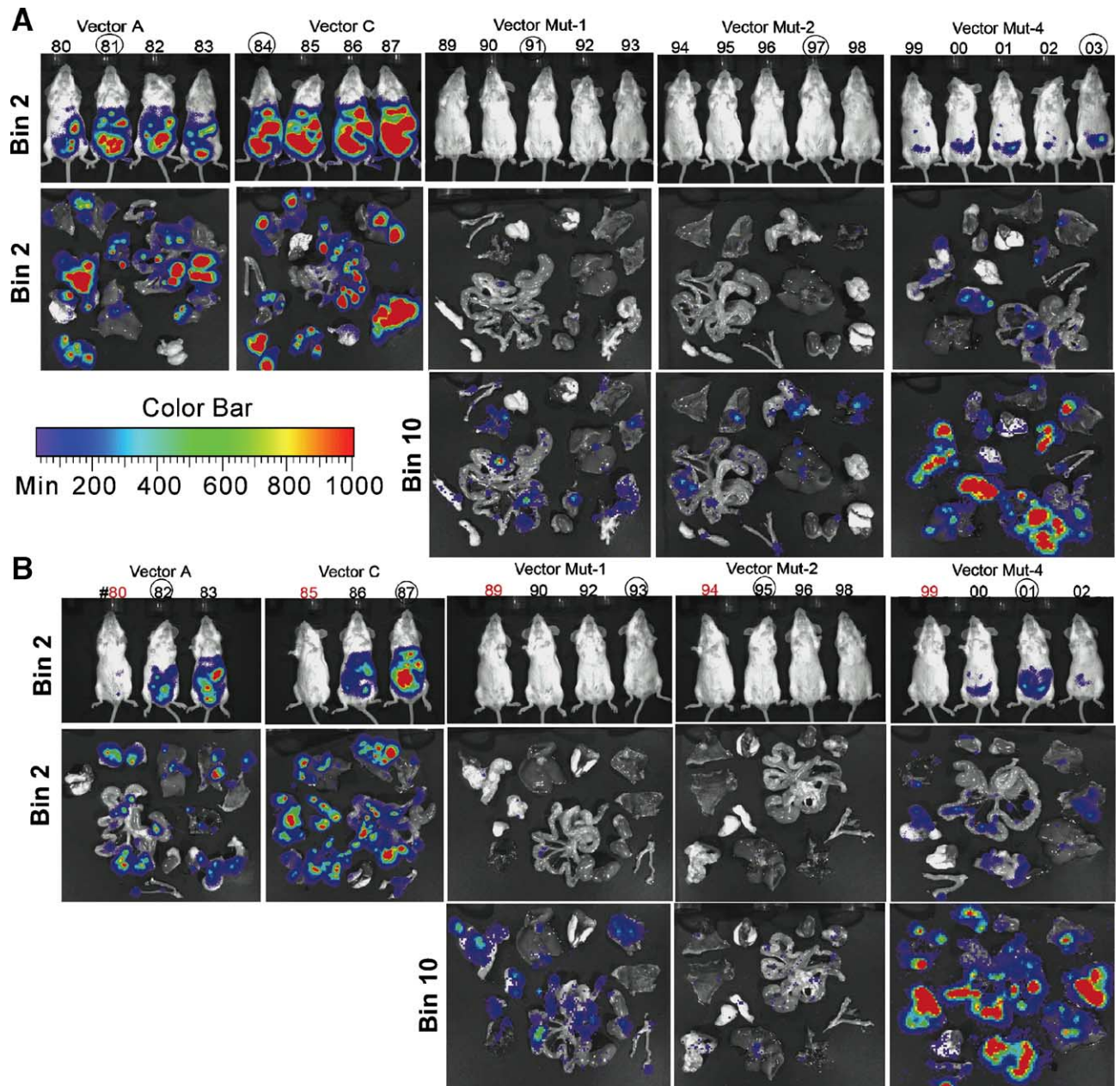


FIG. 6. Tumor targeting of Ar-339 E2 mutants. (A) SCID female mice were injected ip on day 0 with 2×10^6 ES-2 cells/mouse. On day 4, five mice per group were injected ip with one dose of vector A (JT-BB/SP6-RFluc, 10^5 TU/ml), vector C (SP6-H/SP6-RFluc, 10^3 TU/ml), Mut-1 (SP6-HK70/SP6-RFluc, 10^3 TU/ml), Mut-2 (SP6-HK70V251/SP6-RFluc, 10^4 TU/ml), or Mut-4 (SP6-HI3K70E181V251/SP6-RFluc, 10^4 TU/ml) and the next day (day 5) IVIS-imaged for vector luciferase signal. The peritoneum was removed and the organs were harvested and imaged. For the three mutants, IVIS images at Bin10 resolution were taken of organ arrays. Only at this high sensitivity did some mice of the Mut-1 and Mut-2 groups show very low residual signal in metastatic implants (lower images). (B) Some mice per group received a second ip injection of the vectors on day 6, and peritoneal cavities and organs were imaged on day 7. One mouse per group (Nos. 80, 85, 89, 94, and 99) was not injected to serve as a luciferase background control. For the three E2 mutants, high-sensitivity Bin10 images were also taken. Vectors showed infection patterns equivalent to those of the first injection. For both A and B the image scale was whole body at Bin2 min 30, max 10^3 counts/pixel and organ arrays at Bin2 and Bin 10 min 20, max 10^3 counts/pixel. Organs correspond to mice indicated with a circled number.

comparable to that of Sindbis virus. The viral spike is composed of three E1–E2 heterodimers that lean against each other and has a gap between the base of neighboring E1–E2 heterodimers that would allow E2 to move out of the center of the spike during fusion [15]. These data suggest that there is structural flexibility in this area of the spike; therefore, alterations in residue 70 should not be critical for mutant vectors' stability *in vivo*. In addition, previous studies with stable deletion mutants in the E2 receptor-binding domain also showed equivalent *in vitro* titers but drastic reduction of infectivity in live *Aedes aegypti* mosquitoes [22]. The loss of vector infectivity would be more likely to occur via a decrease in cell receptor binding affinity, especially *in vivo*, where the environmental conditions for vector infection are more restrictive.

The high-affinity laminin receptor has been described as the cell surface receptor for Sindbis virus [23]. Laminin receptor also mediates cellular interaction with extracellular matrix. In tumors it is overexpressed compared to normal cells [24–30], which would allow wild-type Sindbis vector to target *in vivo* tumors easily. In the presence of the extracellular matrix, the Mut-1 and Mut-2 vectors, however, may have a lower affinity for the receptor due to competition with laminin receptor binding proteins. Further studies of mutants in the viral spike should lead to a better understanding of the mechanisms used by Sindbis vectors to target and infect tumors *in vivo*.

MATERIALS AND METHODS

Sindbis cDNA cloning. Sindbis virus strain Ar-339 was obtained from the American Type Culture Collection (Manassas, VA, USA; No. VR-68) and propagated on a secondary CEF cell line. Total RNA from infected CEFs was extracted with TRIzol (Invitrogen, San Diego, CA, USA) following the manufacturer's protocol. Sindbis virus genome was cloned in six overlapping fragments: cDNA-1, cDNA-2, C3A, C3B, cDNA-4, and cDNA-5. Primers were designed to take advantage of unique restriction sites of the virus; their sequences are shown in Supplementary Table 1. In primer SV-C3R the restriction endonuclease recognition site *Xba*I was introduced to allow cDNA-3 construction. The cloning procedure was the same for all fragments except for PCR cycle conditions. To avoid mutations due to RT or polymerase chain reactions, for each plasmid three different RT reactions were made and each one served as a template for one Pfx-PCR. The three PCR-amplified bands of each fragment were cloned separately into pCR4Blunt-TOPO plasmid (Invitrogen) following the manufacturer's protocol and sequenced (Skirball Institute of Biomolecular Medicine, NYU). RT reactions were performed with 5 µg total RNA from infected cells with ThermoScript RNase H⁻ reverse transcriptase (Invitrogen), and the Pfx-PCRs were performed with Platinum Pfx DNA polymerase (Invitrogen), in both cases following the manufacturer's instructions. Cycle conditions for each fragment are summarized in Supplementary Table 2. The cDNA3_Topo was engineered by cloning the *Hpa*I/*Sac*I 774-bp C3B_Topo fragment into the *Hpa*I/*Sac*I C3A_Topo vector.

Ar-339 plasmid construction. To construct the Ar-339 vectors, the Sindbis genome was split into two plasmids: the replicon, containing Sindbis replicase and viral subgenomic promoter, and the helper, carrying the viral subgenomic promoter, capsid, and envelope protein sequences. The first step was to generate an SP6 polylinker in two fragments, using primers Poly1-SP6(+)/Poly2(-) for the 5' end containing the SP6

promoter and 3'-end primers Poly-3(+)/Poly-4(-) with a multicloning site; sequences of the primers are given in Supplementary Table 3. The SP6 polylinker fragments were ligated at the *Xba*I site and cloned into the *Afl*III/*Aat*II site of the pUC vector, containing the *Escherichia coli* replication origin and ampicillin resistance gene. The Sindbis virus 3' end from nt 11392 to 11694 was obtained by Pfx-PCR on plasmid cDNA-5_Topo with primers PolyA-F and PolyA-R (Supplementary Table 3) and cycle conditions of 94°C for 5 min; 35 cycles of 94°C for 45 s; 53.2°C for 30 s, and 72°C for 45 s; and 72°C for 1 min. The fragment was cloned into the *Hpa*I site of the SP6-pUC plasmid to generate the SP6-pUC-PolyA plasmid. To construct the SP6-R plasmid, viral cDNA fragments from cDNA_Topo vectors were cloned sequentially in SP6-PolyA using restriction sites *Mfe*I and *Bgl*II for cDNA-1, *Avr*II/*Bgl*II for cDNA-2, and *Xba*I/*Avr*II for cDNA-3. The SP6-H helper plasmid was engineered by first cloning Sindbis virus nt 1 to 425 into the SP6-pUC-PolyA plasmid. Then, both *Bam*HI/*Bcl*I cDNA-4 and *Bcl*I/*Nsi*I cDNA-5 were ligated to the previously constructed plasmid.

SP6-HE2 mutants. Mutants were engineered from the SP6-H plasmid using the Quick Change IIx site-directed mutagenesis kit (Stratagene, La Jolla, CA, USA) and primers E2-I3-F/E2-I3-R or E2-K70-F/E2-K70-R or E2-E181-F/E2-E181-R or E2-V251-F/E2-V251-R (Supplementary Table 4). The 1270-bp *Bss*HII/*Ban*II fragment of each clone, containing the mutation, was subcloned into plasmid SP6-H and sequenced.

Reporter gene cloning in replicon plasmids. The firefly luciferase gene was excised at the *Nhe*I/*Xba*I sites from the pGL3 plasmid (Promega, Madison, WI, USA) and cloned into the *Xba*I site of the replicon SP6-R, to generate SP6-RFluc. The *Renilla* luciferase gene from plasmid pRL-CMV (Promega) was similarly cloned to generate the SP6-RhRluc plasmid.

Cells. The CEF cell line was a gift from Dr. Martinez-Sobrido (Mount Sinai School of Medicine, New York, NY, USA) and was cultured in EMEM (Fisher Scientific, Morris Plains, NJ, USA) supplemented with 10% fetal bovine serum, NaHCO₃ 1.5 g/L, L-glutamine 292 mg/L, and penicillin/streptomycin 100 U/ml. BHK and ES-2 cells were obtained from the American Type Culture Collection. BHK cells were maintained in αMEM (JRH Bioscience, Lenexa, KS, USA) with 5% FBS. ES-2 cells were cultured in McCoy's 5A medium (Mediatech, Inc., Herndon, VA, USA) supplemented with 10% fetal bovine serum. ES-2/Fluc cells were derived from the ES-2 line by stable transfection of a plasmid, pIRES2-Fluc/EGFP, as described previously [3].

Viral vector preparation. The plasmids carrying the Sindbis replicon or Sindbis helper sequences were linearized with *Pac*I, *Not*I, or *Xho*I, before *in vitro* transcription using the SP6 mMACHINE RNA transcription kit (Ambion, Austin, TX, USA) following the manufacturer's protocol. Viral vectors were generated by coelectroporation of *in vitro*-transcribed RNAs from replicon and helper plasmids into BHK cells. The titers of Sindbis virus vectors were assayed in BHK-21, ES-2, or ES-2/Fluc cells as described previously [3,8]. Briefly, supernatants from coelectroporated BHK-21 cells containing viral particles were collected and serially diluted to infect 2 × 10⁵ cells/dilution, for 1 h at room temperature. Then the cells were washed with PBS and incubated with 2 ml of medium at 37°C for 24 h. Cell lysates were then assayed for firefly or *Renilla* luciferase activity using the Steady-Glo Luciferase Assay System or the *Renilla* Luciferase Assay System (Promega). Vector titers refer to the number of infectious particles or transducing units per milliliter of supernatant and were estimated as the last dilution having detectable reporter activity.

Animal models. All animal experiments were done in accordance with NIH and institutional guidelines. To determine the therapeutic effects of Sindbis virus vectors, SCID mice (female, 6–8 weeks of age; Taconic) were intraperitoneally injected with 1.5 × 10⁶ ES-2/Fluc cells/mouse and from day 5 treated daily with ~10⁶ TU of Sindbis vectors in 0.5 ml Opti-MEM I/mouse. Disease progression was determined by IVIS imaging on days 1, 5, 9, and 13 using the IVIS Imaging System 100 Series (Xenogen Corp., Alameda, CA, USA) as described previously [3]. Survival curves were compared with log rank test. All the *P* values presented in this study are two-tailed. Statistical analyses were performed using Prism 3.0 cx (GraphPad Software). For colocalization experiments, two SCID mice/vector

(female, 6–8 weeks of age; Taconic) were inoculated ip with 1.5×10^6 ES-2/Fluc cells on day 0 and received one ip treatment of vector C ($\sim 10^6$ TU in 0.5 ml of Opti-MEM I) on day 5. The next day (day 6), mice were injected ip with 0.3 ml of 0.2 mg/ml coelenterazine (Biotium, Inc., Hayward, CA, USA) followed by IVIS imaging for the *Renilla* luciferase vector activity. Thirty minutes later, the same mice were injected ip with 0.3 ml of 15 mg/ml D-luciferin (Biotium, Inc.) and a second IVIS imaging for ES-2/Fluc firefly luciferase activity was performed. Sindbis Ar-339 vector targeting experiments were done in two groups of SCID mice (female, 6–8 weeks of age; Taconic) with five mice per vector group: one without tumor induction and the second one with induced tumors. The tumor-free animals were injected ip with vectors carrying the firefly luciferase reporter gene on day 0, imaged by IVIS on day 1, received a second injection of vectors on day 2, and on day 3 were IVIS-imaged again. For the second group, SCID female mice were injected ip on day 0 with 2×10^6 ES-2 cells/mouse and on day 4 mice were injected with the same vectors. After the first whole-body IVIS imaging on day 1, the peritoneum was removed for another IVIS imaging of the peritoneal cavity. The remaining mice of the group, except one for background control, had a second ip injection of vectors on day 6 and were imaged again on day 7.

Tissue sections and slide preparation. Hematoxylin and eosin staining of tissue sections was performed as described previously [3]. Immunohistochemistry for luciferase was performed on formalin-fixed paraffin-embedded tissues. Five-micrometer-thick tissue sections were placed onto charged glass slides and deparaffinized through washes of xylene, graded alcohol (100–70%), and deionized water. Immunostains were performed on an automated immunostainer, NexES (Ventana Medical Systems, Tucson, AZ, USA) with a primary polyclonal goat anti-luciferase antibody (Promega) at a dilution of 1:50 (protein concentration 1 mg/ml). Biotinylated secondary mouse anti-goat antibody was used at a dilution of 1:100. Detection was via the generation of an avidin–biotin horseradish peroxidase complex using 3,3'-diaminobenzidine as the chromagen. Hematoxylin was used as a counterstain and sections following dehydration were mounted using Permount.

ACKNOWLEDGMENTS

We thank Dr. Angel Pellicer (New York University School of Medicine) for critically reading the manuscript and for helpful discussions and Dr. Luis Martinez-Sobrido (Mount Sinai School of Medicine) for the kind gift of CEF cells. This study was supported by U.S. Public Health Service Grants CA22247, CA100687, and CA68498 from the National Cancer Institute, National Institutes of Health, Department of Health and Human Services; by U.S. Army Grant OC000111; and by a generous gift from the Karan-Weiss Foundation.

RECEIVED FOR PUBLICATION MARCH 7, 2005; REVISED JUNE 23, 2005; ACCEPTED JUNE 27, 2005.

APPENDIX A. SUPPLEMENTARY DATA

Supplementary data associated with this article can be found, in the online version, at doi:10.1016/j.jymthe.2005.06.476.

REFERENCES

1. Strauss, J. H., and Strauss, E. G. (1994). The alphaviruses: gene expression, replication, and evolution. *Microbiol. Rev.* **58**: 491–562.
2. Tseng, J. C., et al. (2004). Using Sindbis viral vectors for specific detection and suppression of advanced ovarian cancer in animal models. *Cancer Res.* **64**: 6684–6692.
3. Tseng, J. C., et al. (2004). Systemic tumor targeting and killing by Sindbis viral vectors. *Nat. Biotechnol.* **22**: 70–77.
4. Taylor, R. M., and Hurlbut, H. S. (1953). The isolation of coxsackie-like viruses from mosquitoes. *J. Egypt. Med. Assoc.* **36**: 489–494.
5. Hurlbut, H. S. (1953). The experimental transmission of a coxsackie-like virus by mosquitoes. *J. Egypt. Med. Assoc.* **36**: 495–498.
6. Frothingham, T. E. (1955). Tissue culture applied to the study of Sindbis virus. *Am. J. Trop. Med. Hyg.* **4**: 863–871.
7. Burge, B. W., and Pfefferkorn, E. R. (1966). Complementation between temperature-sensitive mutants of Sindbis virus. *Virology* **30**: 214–223.
8. Tseng, J. C., Levin, B., Hirano, T., Yee, H., Pampeno, C., and Meruelo, D. (2002). In vivo antitumor activity of Sindbis viral vectors. *J. Natl. Cancer Inst.* **94**: 1790–1802.
9. Strauss, E. G., Rice, C. M., and Strauss, J. H. (1984). Complete nucleotide sequence of the genomic RNA of Sindbis virus. *Virology* **133**: 92–110.
10. Wang, H. L., O'Rear, J., and Stollar, V. (1996). Mutagenesis of the Sindbis virus nsP1 protein: effects on methyltransferase activity and viral infectivity. *Virology* **217**: 527–531.
11. Rikonen, M., Peranen, J., and Kaariainen, L. (1994). ATPase and GTPase activities associated with Semliki Forest virus nonstructural protein nsP2. *J. Virol.* **68**: 5804–5810.
12. Geigenmuller-Gnirke, U., Nitschko, H., and Schlesinger, S. (1993). Deletion analysis of the capsid protein of Sindbis virus: identification of the RNA binding region. *J. Virol.* **67**: 1620–1626.
13. Owen, K. E., and Kuhn, R. J. (1996). Identification of a region in the Sindbis virus nucleocapsid protein that is involved in specificity of RNA encapsidation. *J. Virol.* **70**: 2757–2763.
14. Lee, H., and Brown, D. T. (1994). Mutations in an exposed domain of Sindbis virus capsid protein result in the production of noninfectious virions and morphological variants. *Virology* **202**: 390–400.
15. Zhang, W., Mukhopadhyay, S., Pletnev, S. V., Baker, T. S., Kuhn, R. J., and Rossmann, M. G. (2002). Placement of the structural proteins in Sindbis virus. *J. Virol.* **76**: 11645–11658.
16. Li, M. L., Liao, H. J., Simon, L. D., and Stollar, V. (1999). An amino acid change in the exodomain of the E2 protein of Sindbis virus, which impairs the release of virus from chicken cells but not from mosquito cells. *Virology* **264**: 187–194.
17. Bhaumik, S., and Gambhir, S. S. (2002). Optical imaging of *Renilla* luciferase reporter gene expression in living mice. *Proc. Natl. Acad. Sci. USA* **99**: 377–382.
18. McKnight, K. L., et al. (1996). Deduced consensus sequence of Sindbis virus strain AR339: mutations contained in laboratory strains which affect cell culture and in vivo phenotypes. *J. Virol.* **70**: 1981–1989.
19. Ohno, K., Sawai, K., Iijima, Y., Levin, B., and Meruelo, D. (1997). Cell-specific targeting of Sindbis virus vectors displaying IgG-binding domains of protein A. *Nat. Biotechnol.* **15**: 763–767.
20. Dubuisson, J., and Rice, C. M. (1993). Sindbis virus attachment: isolation and characterization of mutants with impaired binding to vertebrate cells. *J. Virol.* **67**: 3363–3374.
21. Sammels, L. M., Lindsay, M. D., Poidinger, M., Coelen, R. J., and Mackenzie, J. S. (1999). Geographic distribution and evolution of Sindbis virus in Australia. *J. Gen. Virol.* **80**(Pt 3): 739–748.
22. Myles, K. M., Pierro, D. J., and Olson, K. E. (2003). Deletions in the putative cell receptor-binding domain of Sindbis virus strain MRE16 E2 glycoprotein reduce midgut infectivity in *Aedes aegypti*. *J. Virol.* **77**: 8872–8881.
23. Wang, K. S., Kuhn, R. J., Strauss, E. G., Ou, S., and Strauss, J. H. (1992). High-affinity laminin receptor is a receptor for Sindbis virus in mammalian cells. *J. Virol.* **66**: 4992–5001.
24. Barsky, S. H., Rao, C. N., Hyams, D., and Liotta, L. A. (1984). Characterization of a laminin receptor from human breast carcinoma tissue. *Breast Cancer Res. Treat.* **4**: 181–188.
25. Liebman, J. M., Burbelo, P. D., Yamada, Y., Fridman, R., and Kleinman, H. K. (1993). Altered expression of basement-membrane components and collagenases in ascitic xenografts of OVCA-3 ovarian cancer cells. *Int. J. Cancer* **55**: 102–109.
26. Liotta, L. A., Horan, P., Rao, C. N., Bryant, G., Barsky, S. H., and Schlom, J. (1985). Monoclonal antibodies to the human laminin receptor recognize structurally distinct sites. *Exp. Cell Res.* **156**: 117–126.
27. Liotta, L. A., Rao, N. C., Barsky, S. H., and Bryant, G. (1984). The laminin receptor and basement membrane dissolution: role in tumour metastasis. *Ciba Found. Symp.* **108**: 146–162.
28. Terranova, V. P., Rao, C. N., Kalebic, T., Margulies, I. M., and Liotta, L. A. (1983). Laminin receptor on human breast carcinoma cells. *Proc. Natl. Acad. Sci. USA* **80**: 444–448.
29. van den Brule, F. A., et al. (1994). Differential expression of the 67-kD laminin receptor and 31-kD human laminin-binding protein in human ovarian carcinomas. *Eur. J. Cancer* **30A**: 1096–1099.
30. van den Brule, F. A., et al. (1996). Expression of the 67 kD laminin receptor in human ovarian carcinomas as defined by a monoclonal antibody, MLu5. *Eur. J. Cancer* **32A**: 1598–1602.